molecular pharmaceutics

ARTICLE

pubs.acs.org/molecularpharmaceutics

PET of Insulinoma Using ^{18}F-FBEM-EM3106B, a New GLP-1 Analogue

Haokao Gao,[†,‡] Gang Niu,[†] Min Yang,[†] Qimeng Quan,[†] Ying Ma,[†] Eunice N. Murage,[§] Jung-Mo Ahn,[§] Dale O. Kiesewetter,[*,†] and Xiaoyuan Chen[*,†]

[†]Laboratory of Molecular Imaging and Nanomedicine (LOMIN), National Institute of Biomedical Imaging and Bioengineering (NIBIB), National Institutes of Health (NIH), Bethesda, Maryland 20892, United States

[‡]Department of Cardiology, Xijing Hospital, The Fourth Military Medical University, Xi'an 710032, China

[§]Department of Chemistry, University of Texas at Dallas, Richardson, Texas 75080, United States

ABSTRACT: Derived from endocrine pancreatic beta cells, insulinomas express glucagon-like peptide-1 (GLP-1) receptor with high density and incidence. In this study, we labeled a novel GLP-1 analogue, EM3106B, with ^{18}F and performed PET imaging to visualize insulinoma tumors in an animal model.

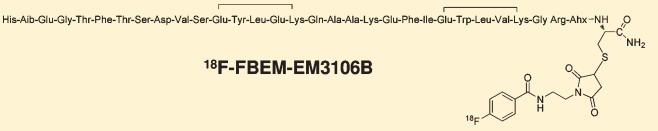

A GLP-1 analogue that contains multiple lactam bridges, EM3106B, was labeled with ^{18}F through a maleimide-based prosthetic group, *N*-2-(4-^{18}F-fluorobenzamido)ethylmaleimide (^{18}F-FBEM). The newly developed radiotracer was characterized by cell based receptor-binding assay, cell uptake and efflux assay. The stability in serum was evaluated by radio-HPLC analysis. *In vivo* PET imaging was performed in nude mice bearing subcutaneous INS-1 insulinoma tumors and MDA-MB-435 tumors of melanoma origin. *Ex vivo* biodistribution study was performed to confirm the PET imaging data. EM3106B showed high binding affinity (IC_{50} = 1.38 nM) and high cell uptake (5.25 ± 0.61% after 120 min incubation). ^{18}F-FBEM conjugation of EM3106B resulted in high labeling yield (24.9 ± 2.4%) and high specific activity (>75 GBq/μmol at the end of bombardment). EM3106B specifically bound and was internalized by GLP-1R positive INS-1 cells. After intravenous injection of 3.7 MBq (100 μCi) of ^{18}F-FBEM-EM3106B, the INS-1 tumors were clearly visible with high contrast in relation to the contralateral background on PET images, and tumor uptake of ^{18}F-FBEM-EM3106B was determined to be 28.5 ± 4.7 and 25.4 ± 4.1% ID/g at 60 and 120 min, respectively. ^{18}F-FBEM-EM3106B showed low uptake in MB-MDA-435 tumors with low level of GLP-1R expression. Direct tissue sampling biodistribution experiment confirmed high tracer uptake in INS-1 tumors and receptor specificity in both INS-1 tumor and pancreas. In conclusion, ^{18}F-FBEM-EM3106B exhibited GLP-1R-receptor-specific targeting properties in insulinomas. The favorable characteristics of ^{18}F-FBEM-EM3106B, such as high specific activity and high tumor uptake, and high tumor to nontarget uptake, demonstrate that it is a promising tracer for clinical insulinoma imaging.

KEYWORDS: insulinoma, glucagon-like peptide-1 receptor, bicyclic GLP-1 analogue, ^{18}F-FBEM, PET

INTRODUCTION

Insulinomas are tumors derived from endocrine pancreatic beta cells. Insulinomas produce insulin in a manner not regulated by blood glucose level and lead to hypoglycemia and related symptoms. These symptoms can be manifested by relatively small tumors. Surgery is the therapy of choice but requires exact anatomical localization of the tumor. Due to the small size (<2 cm) of 90% of insulinomas, it is challenging to precisely diagnose and localize the tumors with conventional imaging methods, such as ultrasonography, computed tomography (CT), or magnetic resonance imaging (MRI).[1,2] Scintigraphy using somatostatin receptor targeting probes has been considered the most sensitive method for the detection of endocrine gastro-enteropancreatic tumors.[3] However, radiolabeled somatostatin is not suitable for insulinoma localization, because of the relatively low expression of somatostatin receptor subtype 2 (sstr2) and subtype 5 (sstr5) on this type of tumor.[4] Arterial stimulation with calcium injection and venous sampling (ASVS) of the insulin released is an important technique for localizing insulinoma. Although ASVS has improved sensitivity and is able to localize over 90% of insulinomas,[5] its application is also limited because of its invasive nature and the risk of complications.[6]

Glucagon-like peptide-1 (GLP-1) receptor is expressed in human insulinomas, especially in benign insulinoma, with high density and incidence.[7] Thus, the receptor provides a very promising target for imaging and therapy, using receptor-avid radioligands. So far, several GLP-1 receptor-avid radioligands have been developed and evaluated in preclinical insulinoma studies. For example, ^{123}I-GLP-1(7−36) amide and ^{123}I-exendin-3 have shown high accumulation in a mouse model bearing a subcutaneously implanted rat insulinoma tumor (RINm5F).[8] However, the relatively low uptake of ^{123}I-exendin-3, due to washout of the radionuclide after internalization and the low peptide stability of ^{123}I-exendin-3, has limited its clinical use. Using [Lys^{40}(6-aminohexanoic acid[Ahx]-DTPA-^{111}In)NH_2]-exendin-4, Wild and his colleagues[9] successfully localized small insulinomas in the Rip1Tag2 spontaneous insulinoma mouse model. With the same animal model, administration of a therapeutic dose of ^{111}In-labeled [Lys^{40}(DTPA)]-exendin-4 markedly inhibited the growth

Received: March 19, 2011
Accepted: July 29, 2011
Revised: July 18, 2011
Published: July 29, 2011

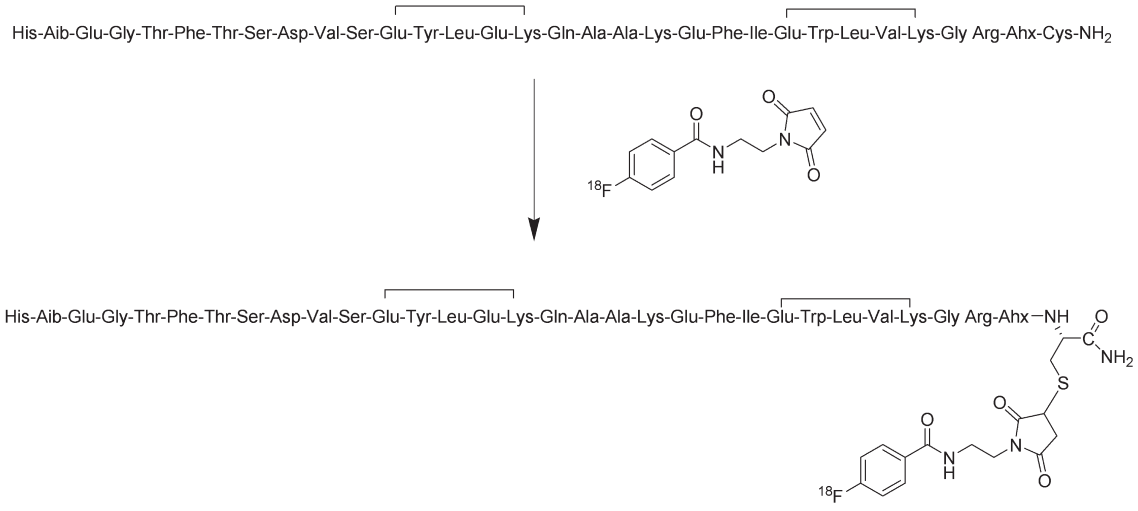

Figure 1. Schematic EM3106B structure and ^{18}F-FBEM radiolabeling.

of insulinomas.[10] The resulting clinical trials with ^{111}In-labeled exendin-4 demonstrated noninvasive localization of insulinomas by single-photon emission computed tomography (SPECT).[11,12] In addition, [Lys^{40}(Ahx-DOTA-^{68}Ga)NH$_2$]-exendin-4 has been evaluated for use in PET imaging and [Lys^{40}(Ahx-hydrazinonicotinamide[HYNIC]-^{99m}Tc/ethylenediaminediacetic acid [EDDA])NH$_2$]-exendin-4 has been evaluated for SPECT.[13]

In order to overcome the rapid degradation of GLP-1 by enzymes like dipeptidyl peptidase-IV (DPP-IV) and neutral endopeptidase (NEP) 24.11, conformationally constrained GLP-1 analogues containing multiple lactam bridges have been developed and synthesized.[14] By stabilizing both α-helices in the N- and C-terminal regions simultaneously, the bridges not only improved the receptor activation capability, but also provided outstanding resistance to metabolism by NEP 24.11.[14] In this study, we labeled the newly designed GLP-1R agonist, EM3106B, with ^{18}F for GLP-1R targeted PET imaging. To the best of our knowledge, this is the first preclinical PET imaging with an ^{18}F labeled GLP-1 peptide analogue for insulinoma imaging.

MATERIALS AND METHODS

General. Unless otherwise specified, all reagents were of analytical grade and were obtained from commercial sources. The novel GLP-1 analogue, EM3106B, was synthesized according to the procedure reported previously.[14] The sequence for EM3106B (calculated m/z 3661, observed 3663) is shown in Figure 1. ^{125}I-GLP-1(7−36) was purchased from Perkin-Elmer. ^{18}F-Fluoride was obtained from the NIH Clinical Center cyclotron facility by proton irradiation of ^{18}O-enriched water. High-performance liquid chromatography (HPLC) employed an Agilent HP1100 system (Agilent, Palo Alto, CA) with diode array UV detection coupled to a Bioscan FC-1000 (Bioscan Inc., Washington, DC) flow-through radioactivity detector. Solvent A was 0.1% TFA in water; solvent B was 0.1% TFA in CH_3CN. A Vydac C_{18} column (4.6 × 250 mm) and a gradient beginning at 25% solvent B was held for 5 min; then a linear gradient to 65% solvent B at 35 min was used with a flow rate of 1 mL/min. Semipreparative HPLC employed a Perkin-Elmer series 200 binary pump coupled to an Agilent HP-1100 variable wavelength UV detector and Bioscan FC-1000 radioactivity detector. A Vydac 9.4 × 250 mm C_{18} column was used with a flow of 5 mL/min. Gradient elution began at 30% B, was held for 5 min, and was followed by a linear gradient to 65% B at 35 min.

Synthesis of FBEM-EM3106B. EM3106B (922 μg, 250 nmol) was dissolved in dimethylformamide (DMF) (20 μL). Degassed phosphate-buffered saline (90 μL) and CH_3CN were added to achieve a homogeneous solution. Then a solution of FBEM (82 μg (313 nmol)/50 μL) was added.[15] The resulting solution was incubated for 60 min at room temperature, diluted with 100 μL 0.1% TFA, and submitted to HPLC purification using the gradient described in the general experimental section. The major peak was collected, the acetonitrile evaporated *in vacuo*, and the water removed by lyophilization. The purity was confirmed on the analytical HPLC system with a peak at 20.5 min at ∼95% purity. Analysis by HPLC−MS (Waters QTOF, Waters Acquity UHPLC, Waters, Milford, MA) gave, after deconvolution for multiply charged species, m/z 3925.002 (calculated: 3922.96).

Radiochemistry. ^{18}F-FBEM (N-(2-(2,5-dioxo-2,5-dihydro-1*H*-pyrrol-1-yl)ethyl)-4-^{18}F-fluorobenzamide) was prepared using an Eckert & Ziegler apparatus as previously described.[15] [^{18}F]FBEM was obtained from the synthesis apparatus in CH_2Cl_2. An aliquot of this solution was evaporated to dryness and redissolved in 10 μL of ethanol. EM3106B (111−135 μg) was first dissolved in 10 μL of DMF and then diluted with 45 μL of PBS (phosphate buffered saline) and 45 μL of CH_3CN. The peptide solution was added to the ethanol solution of ^{18}F-FBEM and allowed to stand at room temperature for 30 min. The reaction mixture was diluted with 50 μL of 0.1% TFA and injected onto the semipreparative Vydac column. The major radioactivity peak eluting at 15.5 min was collected, diluted to 20 mL and trapped on a Varian BondElut (500 mg) cartridge (first activated with 2 mL of ethanol and re-equilibrated with 2 mL of water). The column was washed with water (2 mL) and the product eluted with 1.0−1.5 mL of ethanol (10 mM HCl). The eluate was concentrated to ∼100 μL of ethanol and then diluted as appropriate for the *in vitro* or *in vivo* experiment.

For quality control purposes, a portion of the product was diluted and reinjected onto an analytical Vydac C18 HPLC column to assay for radiochemical purity. The product eluted at 20.7 min. Specific activity was estimated from a calibration curve

at 210 and 230 nm derived from unmodified EM3106B. The estimates from the two wavelengths were averaged for each batch.

Cell Culture and Animal Model. All animal studies were conducted in accordance with the principles and procedures outlined in the Guide for the Care and Use of Laboratory Animals and were approved by the Institutional Animal Care and Use Committee of Clinical Center, NIH. The rat insulinoma cell line INS-1 was grown in RPMI-1640 medium supplemented with 10% fetal bovine serum (FBS), 100 IU/mL penicillin, and 100 μg/mL streptomycin (Invitrogen), and in a humidified atmosphere containing 5% CO_2 at 37 °C. The MDA-MB-435 cell line was purchased from the American Type Culture Collection (ATCC) and grown in Leibovitz's L-15 medium supplemented with 10% (v/v) FBS under a 100% air atmosphere at 37 °C. The cells were harvested by trypsinization with trypsin/EDTA. The INS-1 and MDA-MB-435 tumor models were developed in 5- to 6-week old female athymic nude mice (Harlan Laboratories) by injection of 5×10^6 cells in the left or right front shoulders. Tumor growth was monitored using caliper measurements of perpendicular axes of the tumor. The tumor volume was estimated by the following formula: tumor volume = $a \times b^2/2$, where a and b were the tumor length and width, respectively, in millimeters. The mice underwent small-animal PET studies when the tumor volume reached 100−300 mm^3 (3−4 weeks after inoculation).

Saturation Cell Binding Assay. INS-1 cells were suspended in buffer (PBS supplemented with 2 mM $CaCl_2$, 1 mM $MgCl_2$, and 0.1% BSA) at a cell concentration of 2×10^6 /mL. To each well of a 96-well plate were added buffer, ^{125}I-GLP-1(7−36) (Perkin-Elmer, MA, specific activity 1100 Ci/mmol), and INS-1 cells. GLP-1 was added at 10 different concentrations up to 0.1 μCi (3.7 kBq) per well. Nonspecific binding was determined in a separate set of wells using the same concentration of ^{125}I-GLP-1(7−36) and a 100-fold excess of exendin-4 as competitor. The wells were incubated at room temperature for 1 h on a shaker. The wells were washed with three portions of PBS. The plates were then heated for 15 min to completely dry the membrane. The membranes were punched and counted in a gamma counter. The B_{max} value was determined using GraphPad Prism software and fitting to a one site binding model.

Competitive Cell Binding Assay. INS-1 cells were trypsinized and resuspended in PBS containing 1 mM $CaCl_2$, 5 mM $MgCl_2$, 0.5% (w/v) BSA and 0.3 mM NaN_3. Incubation was conducted with 96-well MultiScreen filter plates (Millipore, MA). For each well, the reaction volume is 200 μL containing 10^5 cells, 20 nCi (0.74 kBq) (around 0.01 nM) of ^{125}I-GLP-1(7−36) and 0−1000 nM unlabeled GLP-1, EM3106B or FBEM-EM3106B. The reaction was incubated for 45 min on a shaker at room temperature. The wells were washed with three portions of PBS. The plates were then heated for 15 min to completely dry the membrane. Cell bound radioactivity was measured using a gamma counter (1480 Wizard 3, Perkin-Elmer). Binding results were expressed as percent of total counts; IC_{50} values were calculated using GraphPad Prism software (GraphPad Software Inc., La Jolla, CA).

Serum and Plasma Stability Studies. Mouse serum or human plasma (Sigma, St. Louis, MO) (200 μL) was treated with ~370 kBq (10 μCi) of ^{18}F-FBEM-3106B and mixed gently. A 50 μL aliquot was removed, and the remaining mixture was incubated at 37 °C. At 30 min and at 60 min another 50 μL aliquot was removed. The aliquot was added to 50 μL of CH_3CN, mixed, and centrifuged at 8000 rpm for 5 min. The supernatant was carefully removed and diluted with 100 μL of saline. The extraction efficiency was determined by the ratio of radioactivity in the supernatant divided by the sum of radioactivity in supernatant and pellet from protein precipitation. The supernatants from 0 and 60 min time points were subjected to HPLC analysis (analytical system described in general experimental). One-minute fractions were collected and subsequently counted in a gamma counter.

Cell Uptake, Internalization, and Efflux Studies. Cell uptake, internalization, and efflux of ^{18}F-FBEM-EM3106B peptide were performed with INS-1 tumor cells. For cell uptake, INS-1 cells were seeded into 24-well plates at a density of 1×10^5 cells per well and incubated with 18.5 kBq (0.5 μCi/5 ng)/well of ^{18}F-labeled tracer at 37 °C for 15, 30, 60, and 120 min with or without an excess of 0.1 M EM3106B. The cells were then washed three times with chilled PBS and lysed with 200 μL of 0.1 M NaOH. For internalization, the percentage of ^{18}F-FBEM-EM3106B activity trapped in the cells was determined after removing ^{18}F-FBEM-EM3106B activity bound to the cell surface by washing three times with an acid buffer (50 mM glycine and 0.1 M NaCl, pH 2.8). For efflux studies, about 18.5 kBq (0.5 μCi)/well of ^{18}F-labeled FBEM-EM3106B was first incubated with INS-1 cells in 24-well plates for 2 h at 37 °C. The cells were washed three times with chilled PBS and allowed to stand with fresh buffer. At various time points, the medium was removed and the cells were washed three times with chilled PBS. The cells were then lysed with 200 μL of 0.1 M NaOH. The cell lysate was collected, and the remaining radioactivity was measured in a γ counter (Wallach Wizard, PerkinElmer, Waltham MA, USA). The cell uptake, internalization and efflux were expressed as the percentage of the added dose (% AD) after decay correction. All experiments were performed twice with triplicate wells.

Fluorescence Staining of GLP-1R. Frozen tumor tissue and pancreas sections (5 μm) were fixed with cold acetone for 20 min and dried in the air for 30 min at room temperature (rt). After being blocked with 2% BSA for 30 min, the sections were incubated with rabbit anti-GLP-1R antibody (1:200; Abcam) for 2 h at rt. After washing with PBS, the sections were further incubated with FITC-conjugated goat anti-rabbit secondary antibodies (1:500; Jackson ImmunoResearch Laboratories, West Grove, PA) for 1 h at rt. After PBS washing (3×), the slides were mounted with medium containing 4′-6-diamidino-2-phenylindole (DAPI) and were observed with an epifluorescence microscope (Olympus, X81) equipped with filter sets for both DAPI (excitation, HQ 360 nm; emission, HQ 460 nm) and fluorescein isothiocyanate (FITC) (excitation, HQ 488 nm; emission, HQ 520 nm). Each experiment was performed in pairs, and the pairs were conducted three times.

MicroPET Imaging. PET scans and image analysis were performed using an Inveon microPET scanner (Siemens Medical Solutions). About 3.7 MBq (100 μCi/0.5 to 1 μg) of ^{18}F-FBEM-EM3106B was administered via tail vein injection under isoflurane anesthesia. Five-minute static PET images were acquired at 1 and 2 h postinjection (p.i.; n = 6/group). For GLP-1R blocking experiment, 300 μg of exendin-4 was coinjected with 3.7 MBq (100 μCi) of ^{18}F-FBEM-EM3106B into INS-1 tumor mice and 5 min static PET images were acquired at 1 h time point (n = 4). The images were reconstructed using a two-dimensional ordered-subset expectation maximization (2D OSEM) algorithm, and no correction was applied for attenuation or scattering. For each scan, regions of interest (ROIs) were drawn over the tumor

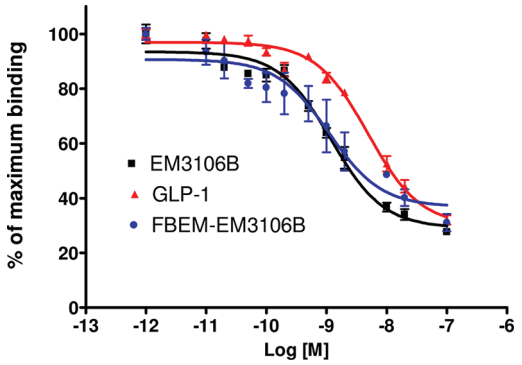

Figure 2. Cell binding assay of EM3106B, FBEM-EM3106 and GLP-1 with INS-1 cells. The IC_{50} values were determined to be 1.25 ± 0.37 nM, 1.07 ± 0.84 nM and 4.92 ± 0.58 nM, respectively.

and major organs using vendor software (ASI Pro 5.2.4.0) on decay-corrected whole-body coronal images. The radioactivity concentrations (accumulation) within the tumors, muscle, liver, and kidneys were obtained from mean pixel values within the multiple ROI volume and then converted to MBq per milliliter per minute using the calibration factor determined for the Inveon PET system. These values were then divided by the administered activity to obtain (assuming a tissue density of 1 g/mL) an image-ROI-derived percent injected dose per gram (% ID/g).

***Ex Vivo* Biodistribution.** Immediately after PET imaging, the tumor-bearing mice were sacrificed and dissected. Blood, tumor, major organs, and tissues were collected and wet-weighed. The radioactivity in the wet whole tissue was measured with a γ-counter (Wallach Wizard, Perkin Elmer). The results were expressed as percentage of injected dose per gram of tissue (% ID/g) for a group of 6 animals. For each mouse, the radioactivity of the tissue samples was calibrated against a known aliquot of the injected radiotracer and normalized to a body mass of 20 g. Values were expressed as mean ± SD.

Statistical Analysis. Quantitative data were expressed as mean ± SD. Means were compared using one-way analysis of variance and Student's *t* test. *P* value of <0.05 was considered statistically significant.

RESULTS

Chemistry and Radiochemistry. A small amount of authentic FBEM-EM3106B was prepared by reaction of 1.25 equiv of nonradioactive FBEM with EM3106B in DMF/CH_3CN/PBS with subsequent HPLC purification. The radiochemical synthesis was conducted in a similar manner. The radiochemical yield based on the product eluted from HPLC and starting ^{18}F-FBEM was 24.8 ± 2.5% (n = 7), uncorrected for decay in a synthesis time of 60 min. Radiochemical purity was 93.0 ± 3.9% (n = 7). The specific activity was 95.6 ± 22.4 GBq/μmol (n = 7; range 75.3 to 139.1 GBq/μmol; 2.1 to 3.7 Ci/μmol) corrected to the end of bombardment (EOB) [22.8 ± 10.0 GBq/μmol at end of synthesis]. With these specific activities, the typical injected doses for *in vivo* imaging studies resulted in a mass dose of 0.5 to 1 μg of peptide at time of injection.

Cell Binding Assay and Serum Stability. The GLP-1 receptor-binding affinity of EM3106B was determined by performing competitive binding assay with ^{125}I-GLP-1(7−36) as the radioligand in GLP-1R positive INS-1 cells. Results of the cell-binding assay were plotted and fitted to sigmoid curves for the

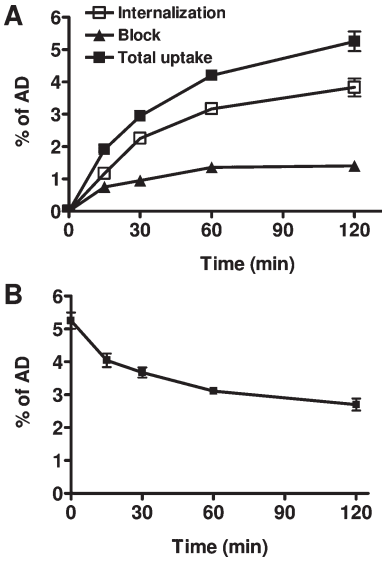

Figure 3. Cell uptake (A) and efflux (B) assay of ^{18}F-FBEM-EM3106B on INS-1 tumor cells. Data were from 2 experiments with triplicate samples and are expressed as mean ± SD. AD, total added dose.

displacement of ^{125}I-GLP-1(7−36) from INS-1 cells. The IC_{50} values for EM3106B, FBEM-EM3106B and GLP-1 were 1.25 ± 0.37 nM, 1.07 ± 0.84 nM and 4.92 ± 0.58 nM, respectively (Figure 2), indicating that EM3106B has higher binding affinity for GLP-1 receptor than GLP-1, which is consistent with a previous report.[14] In addition, FBEM conjugation did not affect the binding affinity of the peptide. B_{max} was determined for our sample of INS-1 cells using a saturation binding assay and ^{125}I-GLP-1(7−36) as the radioligand. The B_{max} was determined to be 6.8 × 10^3 binding sites per cell.

Stability was studied in mouse serum and human plasma. Extraction efficiency from mouse serum was 83.9, 88.7 and 54.2% at 0, 30, and 60 min, respectively. Extraction efficiency from human plasma was 86.2, 77.4, and 67.1% at 0, 30, 60 min, respectively. Recovery from HPLC was >86% in all cases and >80% of the radioactivity eluted in the two consecutive 1 mL fractions at the retention time of the authentic product.

Cell Uptake and Efflux of ^{18}F- FBEM-EM3106B. The cell uptake and efflux of ^{18}F-FBEM-EM3106B were evaluated in INS-1 tumor cells with high levels of GLP-1R. As shown in Figure 3A, 18F-FBEM-EM3106B presented increasing binding to INS-1 cells with time. The total cell uptake values of ^{18}F-FBEM-EM3106B were 1.91 ± 0.21, 2.94 ± 0.21, 4.20 ± 0.23 and 5.25 ± 0.61% after 15, 30, 60, and 120 min incubation, respectively. At the same time, ^{18}F-FBEM-EM3106B also showed a relatively high level of internalization, with 3.17 ± 0.31 and 3.83 ± 0.55% of total input radioactivity internalized after 60 and 120 min incubation, respectively. Inhibition of cell uptake was observed with the presence of 0.1 M EM3106B peptide, confirming the specificity of GLP-1R mediated cell uptake. When the labeled cells were incubated in serum-free medium devoid of radioactivity, ^{18}F-FBEM-EM3106B showed dissociation and efflux from the cells with time (Figure 3B). After 2 h incubation, approximately 50% of the radioactivity was dissociated from the cells.

Immunofluorescence Staining. It has been reported that GLP-1 receptor is mainly expressed in endocrine, nervous, and embryonic tumors.[13] We performed immunofluorescence staining using anti-GLP-1R antibody to observe the expression

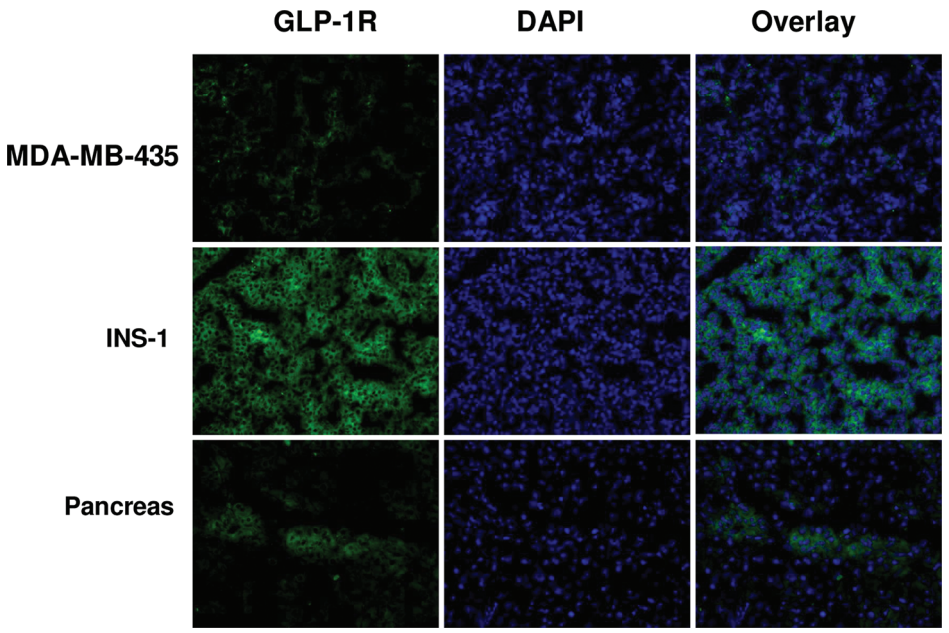

Figure 4. Immunofluorescence staining of GLP-1R expression. The tissue sections were stained with GLP-1R (green) to identify GLP-1R expression and with DAPI (blue) to identify nuclei. A, MDA-MB-435 tumor; B, INS-1 tumor; C, pancreas.

pattern of GLP-1R on tissue sections of INS-1 insolinoma, MDA-MB-435 tumor and pancreas. The results showed strong GLP-1R staining in INS-1 cells and relatively weak staining in MDA-MB-435 cells. The pancreas showed patchy positive fluorescent signal, consistent with the morphological pattern of islets with GLP-1R expression (Figure 4).

MicroPET imaging. Representative coronal microPET images of INS-1 and MB-MDA-435 tumor bearing mice at different times after intravenous injection of 3.7 MBq (100 μCi, mass dose 0.5−1.0 μg) of ^{18}F-FBEM-EM3106B are shown in Figure 5A. The INS-1 tumors, after injection of ^{18}F-FBEM-EM3106B, were clearly visible with high contrast in relation to the contralateral background. The INS-1 tumor uptake of ^{18}F-FBEM-EM3106B was determined to be 28.54 ± 4.74% ID/g at 60 min p.i. (Figure 5B). ^{18}F-FBEM-EM3106B showed very low uptake in MB-MDA-435 tumors, due to the relatively low expression of GLP-1R, with the tumor uptake of only about 1.2% ID/g at 60 min p.i. (Figure 5B).

To further confirm the specificity of the tracer accumulation in INS-1 tumors, we also performed blocking assay by coinjection of about 300 μg of exendin-4 along with ^{18}F-FBEM-EM3106B. At 60 min p.i., the tumor uptake of ^{18}F-FBEM-EM3106B is significantly lower than that of unblocked tumors ($P < 0.001$), indicating that unlabeled peptide efficiently blocked the tumor uptake. Prominent uptake of ^{18}F-FBEM-EM3106B was also observed in the liver and kidneys, with the uptake values calculated to be 8.56 ± 1.61% ID/g for liver and 13.94 ± 1.79% ID/g for kidneys at 60 min p.i., suggesting that this tracer is excreted through both the hepatic and renal-urinary routes

Biodistribution Studies. In order to further confirm the PET imaging quantification, the biodistribution of ^{18}F-FBEM-EM3106B was evaluated in tumor-bearing athymic nude mice immediately after PET imaging. As shown in Figure 6A, the INS-1 tumor uptake of ^{18}F-FBEM-EM3106B was significantly higher than that in the blood and normal organs at the 2 h time point ($P < 0.001$). Consistent with PET imaging data, the INS-1 tumor uptake measured by direct tissue sampling and gamma-counting was 28.32 ± 3.91% ID/g. The tracer accumulations in the kidneys and liver were 29.18 ± 5.14 and 11.92 ± 1.75% ID/g, respectively, at 2 h p.i. The tracer uptake in pancreas was 5.45 ± 0.29% ID/g. The tracer showed only low levels of accumulation in the heart, stomach and intestines, presumably due to low GLP-1R expression in these organs. Blocking experiment showed significantly decreased accumulation of ^{18}F-FBEM-EM3106B in the INS-1 tumor (1.10 ± 0.20% ID/g, $P < 0.001$). In addition, decreases in uptake in the heart, spleen, pancreas, stomach, and intestine were also observed (Figure 6B).

DISCUSSION

In this study, we labeled the newly designed GLP-1R agonist EM3106B with ^{18}F for GLP-1R targeted PET imaging. EM3106B is a conformationally constrained GLP-1 analogue via lactam bridges between residues 18−22 and 30−34 that demonstrated outstanding protection from the degradation by NEP 24.11 in a prior study.[14] Compared to bicyclic GLP-1 analogues previously reported, EM3106B has an unnatural amino acid Aib (2-aminoisobutyric acid) at position 8 to prevent the DPP-IV degradation as demonstrated by taspoglutide that contains two Aib residues in its sequence.[16] Aib at position 8 not only made the peptide stable to DPP-IV but also resulted in higher binding affinity compared to D-Ala as evidenced by our *in vitro* binding experiment. In this study, we prepared the peptide with a C-terminal cysteine residue to allow radiolabeling with the cysteine-specific radiolabeling prosthetic group, FBEM.

Our data show that EM3106B is specifically internalized into insulinoma cells. Compared with the wild-type GLP-1, EM3106B showed higher receptor binding. *In vitro* stability studies of [^{18}F]-FBEM-EM3106B in mouse serum and human plasma stability showed that the extractable radioactivity eluted as a single component. The extraction efficiency decreased with time, suggesting coprecipitation with larger proteins.

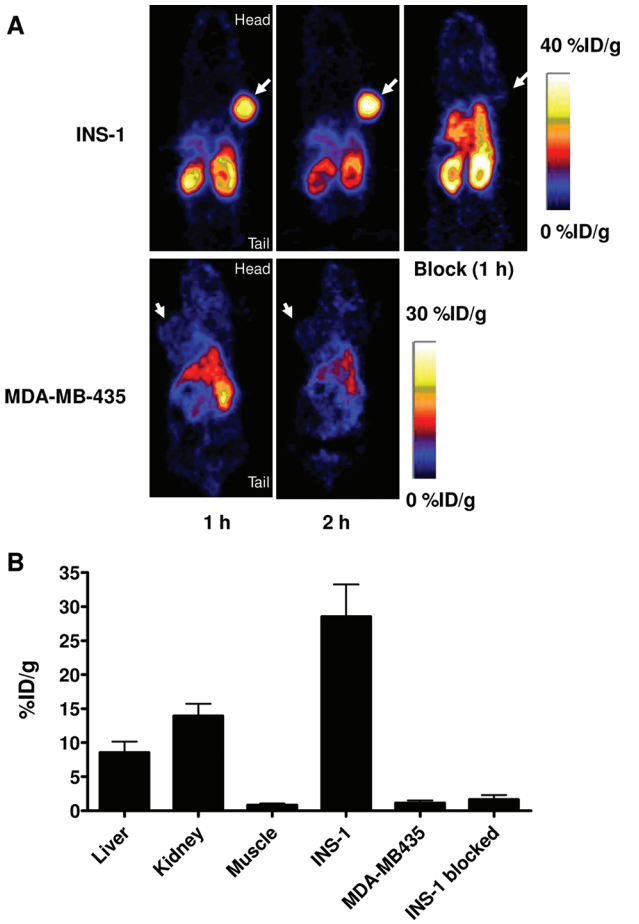

Figure 5. (A) MicroPET whole body images (coronal plane) of athymic nude mice bearing INS-1 or MDA-MB-435 tumors on the shoulder at 1 and 2 h after tail vein injection of 3.7 MBq of ^{18}F-FBEM-EM3106B. Tumors are indicated by white arrows. The displayed plane was selected to best show the tumor cross section. The blocking image was acquired at 1 h following coinjection of 300 μg of exendin-4 and 3.7 MBq of ^{18}F-FBEM-EM3106B. (B) Uptake values at 1 h time point in the kidneys, liver, muscle, INS-1 tumor (blocked and unblocked), and MDA-MB-435 tumor quantified from region of interest (ROI) analysis (n = 6).

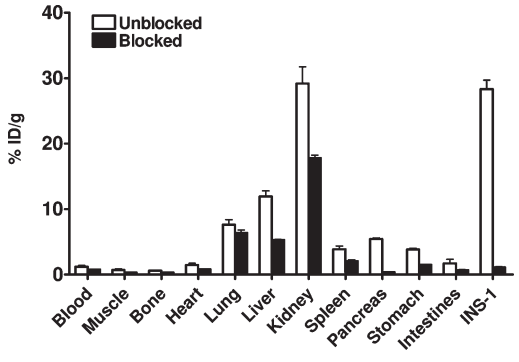

Figure 6. (A) Biodistribution of ^{18}F-FBEM-EM3106B in athymic nude mice bearing subcutaneous INS-1 and MDA-MB-435 tumors after microPET imaging at the 2 h time point (n = 6). (B) Biodistribution of ^{18}F-FBEM-EM3106B in athymic nude mice bearing subcutaneous INS-1 tumors after microPET imaging at the 1 h time point after coinjection of 300 μg of exendin-4 and 3.7 MBq of ^{18}F-FBEM-EM3106B (n = 4).

GLP-1R positive INS-1 tumors were clearly visualized with PET imaging, while MDA-MB-435 tumors with low GLP-1R expression showed much lower tumor uptake of the injected tracer (Figure 5A). The specificity of tracer uptake has been confirmed by blocking assay in which coinjection of unlabeled exendin-4 efficiently blocked INS-1 tumor uptake of ^{18}F-FBEM-EM3106B (Figure 5A,B). Biodistribution analysis was consistent with the PET findings (Figure 6A) and provided the necessary sensitivity to detect blocking of uptake in some tissues with lower uptake (Figure 6B). Blocking studies revealed specific binding in pancreas, spleen, stomach, and intestine. The high tumor uptake of GLP-1R-avid radioligands in insulinoma has been confirmed with several preclinical and clinical studies.[9−11,13,17]

We can compare our results with similar studies in the literature using different tracers for imaging INS-1 tumors. For example, with the same tumor model in Balb/c mice, Brom et al.[17] observed high tumor uptake of both [Lys^{40}(^{111}In-DTPA)]exendin-3 and [Lys^{40}(^{68}Ga-DOTA)]exendin-3. INS-1 tumor uptake was observed to be 8.9% ID/g at 1 h with the Ga-68 tracer and 25% ID/g with the In-111 tracer. The pancreas uptake was 6.7% ID/g and 17.5% ID/g for the Ga-68 tracer and In-111 tracer, respectively. Compared to those published uptakes, we observed uptakes of [^{18}F]FBEM-EM3106B at 2 h of 28.8% ID/g in the INS-1 tumor and 5.45% ID/g in pancreas. These results suggest that [^{18}F]-FBEM-EM3106B is equivalent in potential utility to the previously reported exendin-3 analogues. Blocking studies performed by Brom et al.[17] suggest receptor mediated uptake in tumor, pancreas, stomach, and lung. Our results demonstrate similar specific uptake in these tissues.

The previously published manuscript from Brom et al. also examined cellular uptake as an in vitro marker of affinity.[17] The cell binding component was not equilibrated at 2 h as it continued to increase through 4 h. We limited our study to 2 h because of the relatively shorter half-life of F-18 compared to In-111. Our cell uptake is a sum of both internalized and surface bound radioactivity, while the referenced paper determines surface bound only. The referenced paper shows an internalization of ~1.2 fmol at 2 h and 3.8 fmol at 4 h. Thus at 2 hours the percent internalization was 2.2%. We observe an internalization of 3.83 ± 0.55% with no correction for nonspecific binding. This is also a favorable comparison.

Using the Rip1Tag2 mouse model of pancreatic β-cell carcinogenesis, high tumor uptake of 207 ± 60% ID/g of [Lys^{40}(Ahx-DOTA-^{68}Ga)NH$_2$]-exendin-4 was found at the 2 h time point,[13] while normal pancreas uptake was 16.8 ± 6.3% ID/g at the same time point. These data suggest that the tumors in the Rip1Tag2 mouse model may be much higher in receptor concentration or more highly vascularized to allow much higher uptake of tracer. We expect [^{18}F]FBEM-EM3106 would perform as well or better for imaging in this model system.

However, most imaging studies performed so far have utilized ^{111}In for SPECT imaging or ^{68}Ga for PET imaging. Compared with SPECT, clinical PET offers a higher spatial resolution, sensitivity and imaging contrast. As a generator-derived radionuclide, ^{68}Ga coupling to small biomolecules is potentially an alternative to ^{18}F- and ^{11}C-based analogues. However, a potential disadvantage of ^{68}Ga is the high energy of the emitted β^+ particles limiting the spatial resolution of the images to 3 mm while the intrinsic resolution of the current preclinical PET scanner is 1.5 mm[18] and current clinical scanners have a resolution approaching 4 mm. Since ^{18}F has nearly optimal nuclear decay characteristics for use in PET, including one of the lowest positron

energies, this nuclide has been exploited to develop prosthetic groups for the purpose of radiolabeling peptides.

A high tumor-to-background ratio is a prerequisite for lesion detection by PET/SPECT imaging. Insulinomas originate from pancreatic islet cells and occur primarily in the gastrinoma triangle, defined as the confluence of the cystic and common bile duct, the second and third portions of the duodenum, and the neck and body of the pancreas.[19] Therefore, tumor-to-surrounding-organ ratios, especially with normal pancreas, are important in the application of PET imaging to clinical practice. Our biodistribution study demonstrated that pancreas showed tracer uptake of 5.45 ± 0.29% ID/g, due to native expression of GLP-1R.[20] The tumor-to-pancreas ratio was around 5.3, which predicts an ability to identify insulinoma above the surrounding normal pancreatic background. The high tumor uptake of the tracer also resulted in high tumor-to-background ratios with other normal organs. Although perhaps not relevant to final imaging uses, human lung and kidneys express significantly lower levels of GLP-1 receptor than do those of rat and mice.[21] Thus, our imaging results using a subcutaneous insulinoma tumor model imply a high potential to translate ^{18}F-FBEM-EM3106B into clinical use.

Besides insulinoma detection, another potential application of GLP-1R-avid radioligands is *in vivo* determination of β-cell mass during the course of diabetes development and antidiabetic treatment. [Lys^{40}(Ahx-DTPA-^{111}In)NH$_2$]exendin-4 was used to follow the β-cell viability of an islet transplantation into the forearm of a human patient. One year after the transplantation, focal accumulation of the radiolabeled GLP-1 analogue was observed on planar images.[22] These results depicted clinical evidence that functional human β cells can be imaged *in vivo* with a tracer specific to the GLP-1 receptor. Thus, ^{18}F-FBEM-EM3106B may also have applications for imaging β-cells of pancreatic islets.

CONCLUSIONS

In conclusion, ^{18}F-FBEM-EM3106B showed high binding affinity to GLP-1R and high uptake in insulinomas, resulting in high tumor-to-background ratios. This tracer is expected to have potential for noninvasive PET imaging of insulinomas and the β-cells of pancreatic islets.

AUTHOR INFORMATION

Corresponding Author

*Laboratory of Molecular Imaging and Nanomedicine (LOMIN), National Institute of Biomedical Imaging and Bioengineering (NIBIB), National Institutes of Health (NIH), 31 Center Drive, Suite 1C14, Bethesda, MD 20892-2281, E-mail: shawn.chen@nih.gov; dk7k@nih.gov. Tel: 301-451-4246. Fax: 301-435-4699.

ACKNOWLEDGMENT

This work was supported by the Intramural Research Program (IRP) of the National Institute of Biomedical Imaging and Bioengineering (NIBIB), National Institutes of Health (NIH), Juvenile Diabetes Research Foundation (37-2011-20, Jungmo Ahn), and the International Cooperative Program of the National Science Foundation of China (NSFC) (81028009). G.N. holds an Imaging Sciences Training Fellowship, which is jointly supported by the Radiology and Imaging Sciences Department, NIH Clinical Center and the Intramural Research Program, NIBIB, NIH. We acknowledge the NIH/CC cyclotron facility for isotope production.

REFERENCES

(1) Chatziioannou, A.; Kehagias, D.; Mourikis, D.; Antoniou, A.; Limouris, G.; Kaponis, A.; Kavatzas, N.; Tseleni, S.; Vlachos, L. Imaging and localization of pancreatic insulinomas. *Clin. Imaging* **2001**, *25* (4), 275–83.

(2) Ramage, J. K.; Davies, A. H.; Ardill, J.; Bax, N.; Caplin, M.; Grossman, A.; Hawkins, R.; McNicol, A. M.; Reed, N.; Sutton, R.; Thakker, R.; Aylwin, S.; Breen, D.; Britton, K.; Buchanan, K.; Corrie, P.; Gillams, A.; Lewington, V.; McCance, D.; Meeran, K.; Watkinson, A. Guidelines for the management of gastroenteropancreatic neuroendocrine (including carcinoid) tumours. *Gut* **2005**, *54* (Suppl. 4), iv1–16.

(3) Modlin, I. M.; Tang, L. H. Approaches to the diagnosis of gut neuroendocrine tumors: the last word (today). *Gastroenterology* **1997**, *112* (2), 583–90.

(4) Krenning, E. P.; Kwekkeboom, D. J.; Bakker, W. H.; Breeman, W. A.; Kooij, P. P.; Oei, H. Y.; van Hagen, M.; Postema, P. T.; de Jong, M.; Reubi, J. C.; et al. Somatostatin receptor scintigraphy with [^{111}In-DTPA-D-Phe^1]- and [^{123}I-Tyr^3]-octreotide: the Rotterdam experience with more than 1000 patients. *Eur. J. Nucl. Med.* **1993**, *20* (8), 716–31.

(5) Jackson, J. E. Angiography and arterial stimulation venous sampling in the localization of pancreatic neuroendocrine tumours. *Best Pract. Res., Clin. Endocrinol. Metab.* **2005**, *19* (2), 229–39.

(6) Wiesli, P.; Brandle, M.; Schmid, C.; Krahenbuhl, L.; Furrer, J.; Keller, U.; Spinas, G. A.; Pfammatter, T. Selective arterial calcium stimulation and hepatic venous sampling in the evaluation of hyperinsulinemic hypoglycemia: potential and limitations. *J. Vasc. Interv. Radiol.* **2004**, *15* (11), 1251–6.

(7) Reubi, J. C.; Waser, B. Concomitant expression of several peptide receptors in neuroendocrine tumours: molecular basis for in vivo multireceptor tumour targeting. *Eur. J. Nucl. Med. Mol. Imaging* **2003**, *30* (5), 781–93.

(8) Gotthardt, M.; Fischer, M.; Naeher, I.; Holz, J. B.; Jungclas, H.; Fritsch, H. W.; Behe, M.; Goke, B.; Joseph, K.; Behr, T. M. Use of the incretin hormone glucagon-like peptide-1 (GLP-1) for the detection of insulinomas: initial experimental results. *Eur. J. Nucl. Med. Mol. Imaging* **2002**, *29* (5), 597–606.

(9) Wild, D.; Behe, M.; Wicki, A.; Storch, D.; Waser, B.; Gotthardt, M.; Keil, B.; Christofori, G.; Reubi, J. C.; Macke, H. R. [Lys^{40}(Ahx-DTPA-^{111}In)NH$_2$]exendin-4, a very promising ligand for glucagon-like peptide-1 (GLP-1) receptor targeting. *J. Nucl. Med.* **2006**, *47* (12), 2025–33.

(10) Wicki, A.; Wild, D.; Storch, D.; Seemayer, C.; Gotthardt, M.; Behe, M.; Kneifel, S.; Mihatsch, M. J.; Reubi, J. C.; Macke, H. R.; Christofori, G. [Lys^{40}(Ahx-DTPA-^{111}In)NH$_2$]-Exendin-4 is a highly efficient radiotherapeutic for glucagon-like peptide-1 receptor-targeted therapy for insulinoma. *Clin. Cancer Res.* **2007**, *13* (12), 3696–705.

(11) Wild, D.; Macke, H.; Christ, E.; Gloor, B.; Reubi, J. C. Glucagon-like peptide 1-receptor scans to localize occult insulinomas. *N. Engl. J. Med.* **2008**, *359* (7), 766–8.

(12) Christ, E.; Wild, D.; Forrer, F.; Brandle, M.; Sahli, R.; Clerici, T.; Gloor, B.; Martius, F.; Maecke, H.; Reubi, J. C. Glucagon-like peptide-1 receptor imaging for localization of insulinomas. *J. Clin. Endocrinol. Metab.* **2009**, *94* (11), 4398–405.

(13) Wild, D.; Wicki, A.; Mansi, R.; Behe, M.; Keil, B.; Bernhardt, P.; Christofori, G.; Ell, P. J.; Macke, H. R. Exendin-4-based radiopharmaceuticals for glucagonlike peptide-1 receptor PET/CT and SPECT/CT. *J. Nucl. Med.* **2010**, *51* (7), 1059–67.

(14) Murage, E. N.; Gao, G.; Bisello, A.; Ahn, J. M. Development of potent glucagon-like peptide-1 agonists with high enzyme stability via introduction of multiple lactam bridges. *J. Med. Chem.* **2010**, *53* (17), 6412–20.

(15) Kiesewetter, D. O.; Jacobson, O.; Lang, L.; Chen, X. Automated radiochemical synthesis of [^{18}F]FBEM: A thiol reactive synthon for

radiofluorination of peptides and proteins. *Appl. Radiat. Isot.* **2011**, *69* (2), 410–4.

(16) Sebokova, E.; Christ, A. D.; Wang, H.; Sewing, S.; Dong, J. Z.; Taylor, J.; Cawthorne, M. A.; Culler, M. D. Taspoglutide, an analog of human glucagon-like Peptide-1 with enhanced stability and in vivo potency. *Endocrinology* **2010**, *151* (6), 2474–82.

(17) Brom, M.; Oyen, W. J.; Joosten, L.; Gotthardt, M.; Boerman, O. C. ^{68}Ga-labelled exendin-3, a new agent for the detection of insulinomas with PET. *Eur J. Nucl. Med. Mol. Imaging* **2010**, *37* (7), 1345–55.

(18) Fani, M.; Andre, J. P.; Maecke, H. R. ^{68}Ga-PET: a powerful generator-based alternative to cyclotron-based PET radiopharmaceuticals. *Contrast Media Mol. Imaging* **2008**, *3* (2), 67–77.

(19) Horton, K. M.; Hruban, R. H.; Yeo, C.; Fishman, E. K. Multi-detector row CT of pancreatic islet cell tumors. *Radiographics* **2006**, *26* (2), 453–64.

(20) Ahren, B. Islet G protein-coupled receptors as potential targets for treatment of type 2 diabetes. *Nat. Rev. Drug Discovery* **2009**, *8* (5), 369–85.

(21) Korner, M.; Stockli, M.; Waser, B.; Reubi, J. C. GLP-1 receptor expression in human tumors and human normal tissues: potential for in vivo targeting. *J. Nucl. Med.* **2007**, *48* (5), 736–43.

(22) Pattou, F.; Kerr-Conte, J.; Wild, D. GLP-1-receptor scanning for imaging of human beta cells transplanted in muscle. *N. Engl. J. Med.* **2010**, *363* (13), 1289–90.